



ORIGINAL ARTICLE

Study of complex formation in Al(III) – Gluconic acid system and the influence of UV light on the dissolution and passive behavior of Al

Mohammed A. Amin^{a,b,*}, Moamen S. Refat^{a,c}

^a Materials and Corrosion Lab, Department of Chemistry, Faculty of Science, Taif University, 888 Hawiya, Saudi Arabia

^b Department of Chemistry, Faculty of Science, Ain Shams University, Abbassia, Cairo 11566, Egypt

^c Department of Chemistry, Faculty of Science, Port Said University 42111, Egypt

Received 31 August 2010; accepted 28 September 2010

Available online 6 October 2010

KEYWORDS

Aluminum;
Gluconic acid;
Photo-inhibition of localized corrosion;
Aluminum complexes;
Gluconic acid complexes;
IR-spectroscopy and UV-vis spectra

Abstract The passive and dissolution behavior of Al was studied in 0.25 M gluconic acid solution (HG) under the conditions of continuous illumination (300–400 nm) and non-illumination at 25 °C. Measurements were conducted based on cyclic polarization technique, complemented with SEM examinations. Addition of HG induced localized attack, rather than anodizing, via the formation of Al–gluconate soluble complex species. Complexation with gluconate (G^-) anion was elucidated using elemental analysis, IR-spectroscopy and UV-vis spectra. The infrared spectral data is in agreement with coordination through carboxylate-to-metal, with G^- acting as a monodentate ligand. A little ennoblement in the pitting potential (E_{pit}) was observed for the illuminated electrode (little influence on pit nucleation). On the other hand, the anodic currents at potentials exceeding the pitting potential are greatly reduced upon illumination (significant influence on pit growth and propagation). These findings indicated that the incident photons of the UV light enhanced the resistance of the passive film towards localized attack. These explained in terms of a photo-induced modification of the passive film formed on the anode surface, which render it more resistant to the onset of attack. The repassivation potential (E_{rp}), however, was found to be independent of

* Corresponding author at: Department of Chemistry, Faculty of Science, Ain Shams University, Abbassia, Cairo 11566, Egypt. Tel.: +20 222509331.

E-mail address: maaismail@yahoo.com (M.A. Amin).



the energy of the incident UV light. SEM images revealed that the severity of localized attack was suppressed upon illumination.

© 2010 King Saud University. Production and hosting by Elsevier B.V. All rights reserved.

1. Introduction

Two types of anodic oxide films can be formed in anodization processes on an aluminum sample: barrier and porous (Bocchetta et al., 2002). The type of oxide film is primarily determined by the type of electrolyte. The compact, barrier oxide films on aluminum are formed by anodization, mostly under constant-current (galvanostatic) conditions, in electrolytes which possess significant buffering capacity and do not dissolve oxide at all, e.g., neutral boric acid, ammonium borate, ammonium tartrate, citric acid, tartaric acid, malic acid, succinic acid, etc. (Diglee et al., 1969).

Barrier aluminum oxide films exhibit many interesting properties which are of interest for researchers in various scientific and technological areas: physics, chemistry, electronics, etc. (Wernick et al., 1987; Jackson and Cambell, 1976; Ikonopisov, 1975; Tajima, 1977; van Geel et al., 1957; Tajima et al., 1977a,b; Shimizu and Tajima, 1980a,b; Belca et al., 2000; Ikonopisov et al., 1978; Stojadinovic et al., 2006). Porous oxide films are commonly formed by anodization of aluminum samples in acidic aqueous electrolytes, e.g., oxalic acid, sulfuric acid, phosphoric acid, etc. Such films consist of two regions: an outer region of thick porous-type aluminum oxide and a thin, compact inner region lying adjacent to the metal (Abdel Rehim et al., 2002; Kim et al., 1996; Nagayama et al., 1972; Pakes et al., 2003; Suay et al., 2003; Garcia-Vergara et al., 2008).

Indeed, gluconate is a large hydrocarbon oxyanion and Al would be expected to anodize in the presence of this kind of ion. Anodization without pitting occurs in many acid and salt solutions. Recently, our previous studies (Amin et al., 2010a,b) revealed that Al and Al–Cu alloys suffered from severe localized attack in gluconic acid solutions. The aim of the present work is to study the coordination chemistry of the aggressive gluconate anion (G^-) regarding its interaction with Al(III) and the subsequent formation of Al– G^- soluble complex species. For this purpose, elemental analysis, IR-spectroscopy and UV–vis spectra were used. It was also the purpose of the present work to study the photo-inhibition of localized corrosion of Al in HG solutions and the factors affecting the degree of photo-inhibition based on cyclic polarization technique. Morphology of pitting as a function of the energy of the incident photons is also studied.

2. Experimental

The working electrode employed in the present work was made of Al, provided from the Egyptian Aluminum Company, with composition presented elsewhere (Amin et al., 2010a). The investigated Al electrode was cut as cylindrical rods, welded with Cu-wire for electrical connection and mounted into glass tubes of appropriate diameter using Araldite to offer an active flat disc shaped surface of 0.75 cm^2 geometric area for the working electrode, to contact the test solution. The surface pre-treatment of the electrode was carried out by grinding with different grades of emery papers down to 1200 grit. The electrode was then rinsed with acetone, distilled water and finally

dipped in the electrolytic cell. All solutions were freshly prepared from analytical grade chemical reagents using doubly distilled water and were used without further purification.

Gluconic acid solution (0.25 M) was freshly prepared from analytical grade chemical reagents using doubly distilled water and was used without further purification. For each run, a freshly prepared solution as well as a cleaned set of electrodes was used. Each run was carried out in aerated stagnant solutions at the required temperature ($\pm 1^\circ\text{C}$), using water thermostat.

Cyclic polarization measurements were carried out by sweeping linearly the potential from the starting potential into the positive direction at a scan rate of 0.2 mV s^{-1} till the end potential, and then reversed with the same scan rate till the starting potential to form one complete cycle. These experiments were performed in a three electrode PTFE cell equipped with a quartz window to allow irradiation of the test electrode. A saturated calomel electrode (SCE) was used as the reference electrode and a platinum wire, coiled inside the PTFE cell, was used as the auxiliary electrode.

The working electrode was irradiated at wavelengths between 300 and 400 nm using a 150 W UV-enhanced Xe lamp (Oriel model 6254) and a 1/8 monochromator (Oriel model 77250). The incident power density at 300 nm was 400 mW cm^{-2} , giving a photon flux of $6.0 \times 10^{14}\text{ cm}^{-2}$. The photon flux was maintained at approximately this value at each wavelength by adjusting the light intensity at the surface using neutral density filter. Electrochemical experiments were carried out under the conditions of non-illumination and continuous illumination of the working electrode in HG solutions at 25°C .

Electrochemical measurements were performed using Autolab frequency response analyzer (FRA) coupled to an Autolab Potentiostat/Galvanostat (PGSTAT30) with FRA2 module connected to a personal computer. The stabilization period prior to collecting data was 12 h. The open circuit potential of the working electrode was measured as a function of time during this stabilization time. This time was quite sufficient to reach a quasi-stationary value for the open circuit potential. Diffusion of Cl^- into the cell was avoided as previously mentioned in our previous study (Amin et al., 2010a,b).

For morphology of pitting, Al was exposed to pitting attack at a fixed anodic potential beyond E_{pit} , namely 0.20 V(SCE). The Al sample was held at this potential for 5.0 min, and finally washed thoroughly and submitted to 20 min of ultrasonic cleaning in order to remove loosely adsorbed ions. Same experiment was repeated under the conditions of continuous illumination at 300 nm of the incident UV light. Micro-structural features of the pitted surface were analyzed by SEM examinations using Analytical Scanning Electron Microscope JEOL JSM 6390 LA.

3. Results and discussion

3.1. Localized attack and the formation of soluble Al– G^- complex species

It is clear that on positive going scan, the cathodic current density, which corresponds to hydrogen evolution reaction

decreases gradually and reaches a zero value at the corrosion potential (E_{corr}). The anodic response does not involve active/passive transition and a passive region results due to the formation of a protective barrier oxide film. It is obvious that the electrode retains its passivity up to the pitting potential (E_{pit}) when the current rise starts, denoting pit initiation (see region I) and continues even after the potential scan reversal (see region II), because the pitting attack is enhanced after the pit initiation (autocatalytic character of pitting). A current hysteresis loop, characteristic of pitting corrosion phenomena, appears. This loop allows the repassivation potential (E_{rp}) to be determined (Szkłarska-Smialowska, 1986). Repassivation potential corresponds to the potential value below which no pitting occurs and above which pit nucleation begins (Szkłarska-Smialowska, 1986). The location of E_{rp} with respect to E_{corr} is well-defined in the $\log j$ vs E plot (see the inset of Fig. 1). In the present work, E_{rp} is defined as the potential on the reverse scan at which the anodic current becomes zero (i.e., the current changes polarity). It seems that Al finds it difficult to repassivate in this system since the repassivation potential (E_{rp}) locates outside the passive region, resulting in a large hysteresis loop. This means that Al suffers from severe pitting during the reverse scan.

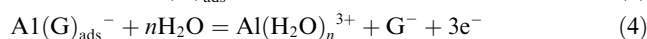
When the repassivation potential is reached, the anodic current density decreases very sharply and rapidly (see region III). The existence of a hysteresis loop in a cyclic potentiodynamic polarization curve indicates a delay in repassivation of an existing pit when the potential is scanned toward negative direction. The larger the hysteresis loop, the more difficult it becomes to repassivate the pit (Szkłarska-Smialowska, 1986).

It is well-known that an oxide or hydroxide surface (M–OH) can become charged by reacting with H^+ or OH^- ions due to surface amphoteric reactions, Eqs. (1) and (2). At low pH, hydroxide surface adsorbs protons to produce positively charged surfaces (M–OH_2^+). At high pH they lose protons to produce negatively charged surfaces (M–O^-).



The number of these sites and the surface charge of the oxide are determined by the pH of the solution. Surface charge influences adsorption of ions from solution and other interfacial phenomena (Brown, 1999). The pH of the potential of zero charge (PZC) for aluminum oxides/hydroxides is between 6 and 9, and in acidic solution, the accumulation of Al–OH_2^+ species accounts for the surface charge (Hohl and Stumm, 1976; Wood et al., 1990). In acidic solution, therefore the positively charged surface sites will electrostatically attract G^- anions. Thus, G^- anions are expected to electrostatically adsorb to rupture the passive oxide film and initiate pitting. Therefore on a passivated electrode, Al dissolution may take place via chemical dissolution of the oxide film stimulated by G^- anions via the formation of Al–G^- soluble complex species (see later).

Gluconate (G^-) is quite a large anion and logically is not expected to occupy anion vacancies, like Cl^- , to initiate pitting corrosion according to the point defect model (PDM). Indeed, we have chosen the localized acidification model to explain why G^- anions induce pitting corrosion to Al (Galvele, 1976a,b; Keitelman et al., 1984). This model assumes that the aggressive anion produces soluble products when it becomes in contact with the metal and that the metal, while corroding in aqueous solutions, reacts with water, producing localized acidification. Based on this model, the adsorption of G^- anions may lead to local dissolution, as shown in the following equations:



where Eq. (4) is the dissolution step and $\text{Al}(\text{H}_2\text{O})_n^{3+}$ represents the solvated Al^{3+} ion. If the rate of oxide film formation is faster than the rates of Eqs. (3) and (4), film healing (passivation) predominates. The converse causes local dissolution (pitting) to dominate. In all probability, if G^- anions adsorb strongly on Al surfaces to promote dissolution, as implied by Eqs. (3) and (4), then these species may be expected to remain bound to the solvated ion to form, as will be shown, a soluble complex species, $\text{Al}(\text{G})_{3(\text{aq})}$ (Eq. (5)).

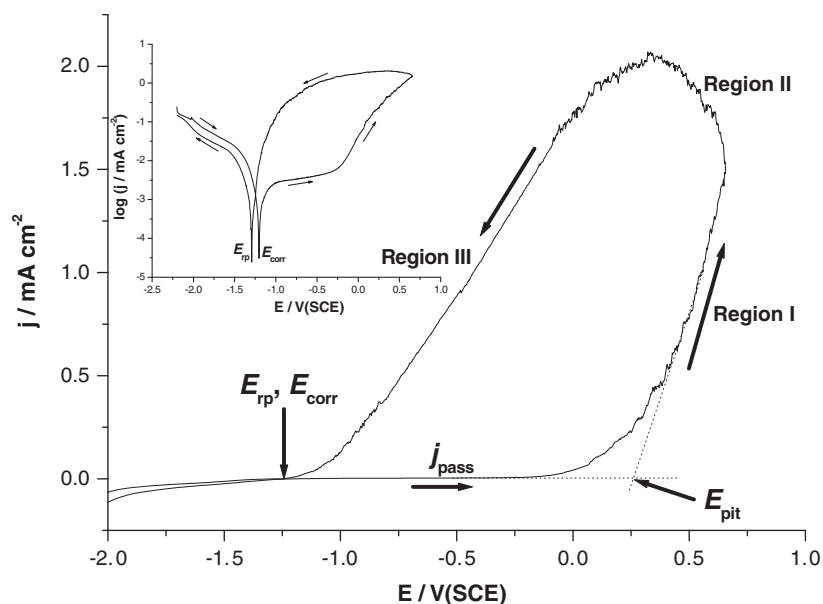
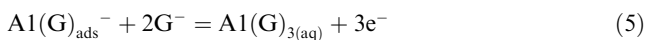


Figure 1 Cyclic polarization curve recorded for Al in 0.25 M HG at a scan rate of 0.2 mV s^{-1} at 25°C .



The onset of passivity breakdown and initiation of pitting corrosion at E_{pit} is now seen to arise as a simple consequence of the dissolution reactions (Eqs. (3) and (4)) and subsequent formation of soluble complex species (Eq. (5)) dominating over the film forming reactions (passivation) at the base of the flaw, resulting in pit formation.

The chemical reaction between the aqueous solution of gluconic acid and Al produced soluble species which upon evaporation gave uncolored solid product. This product is thought to be formed as a result of complexation of Al(III) with free G^- (a good chelating agent), see later. It has been shown that conductivity measurements play an important role in detecting the place of the counter ion with respect to the coordination sphere, i.e., inside or outside (Deacon and Phillips, 1980). This method aids in testing the degree of ionization of the complexes against the free ligands. The higher molar conductance value refers to the presence of the counter ion outside the coordination sphere and vice versa (Deacon and Phillips, 1980).

Results of the present work showed that the conductivity significantly increased from $0.6 \times 10^{-3} \Omega^{-1} \text{cm}^{-1}$ for bare 0.25 M HG solution to $25 \times 10^{-3} \Omega^{-1} \text{cm}^{-1}$ after the complexation process between Al(III) and G^- anion has occurred. These findings suggest that the formed complex can be considered as an electrolyte (i.e., a salt solution). Results of the elemental analysis were found to be in good agreement with the proposed formula of the soluble Al-G $^-$ complex species, namely $\text{Al(G)}_3 \cdot 10\text{H}_2\text{O}$: $\text{Al(G)}_3 \cdot 10\text{H}_2\text{O}$; $M_w = 792 \text{ g mol}^{-1}$: (calc.: C = 9.09%, H = 1.52%; found: C = 8.98%, H = 1.48%).

The main infrared data are summarized in Table 1 and the IR spectra are shown in Fig. 2. The carboxylate group is able to coordinate to metal ions by three different modes: (i) the carboxylate group coordinated to metal ion in a monodentate

Table 1 Main infrared data for (A) HG and (B) $\text{Al(G)}_3 \cdot 10\text{H}_2\text{O}$ (values in cm^{-1}).

(A)	(B)	Assignments
3423 vs,br	3390 s,br	$\nu(\text{OH})$; H_2O νOH ; $-\text{OH}$
2947 sh	3032 sh	$\nu_{\text{as}}(\text{CH}) + \nu_{\text{s}}(\text{CH})$
2870 ms	2767 sh	
	2870 w	
	2856 w	
1735 s	–	$\nu(\text{C}=\text{O})$; COOH
1657 vs		
–	1612 vs	$\nu_{\text{as}}(\text{OCO})$
1412 w	1504 w	$\delta(\text{CH}_2)$
–	1462 ms	$\nu_{\text{s}}(\text{OCO})$
1231 m	1271 s	$\rho_w(\text{CH}_2)$
1151 w	1063 w	$\nu_{\text{as}}(\text{CC})$
1104	938 mw	$\nu_{\text{s}}(\text{CC})$
1088 m	806 ms	$\delta(\text{CC})$
1046 m		
–	728 vw	$\delta(\text{OCO})$
647 w	606 s,br	$\rho_t(\text{H}_2\text{O})$
690 w		$\delta(\text{CCO})$
518 w		$\rho_w(\text{OCO})$
434 w		
–	473 w	$\nu(\text{M}-\text{O})$
	442 vw	

manner when the difference between the wave numbers of the asymmetric and symmetric carboxylate stretching bands ($\Delta\nu = \nu_{\text{as}}\text{COO}^- - \nu_{\text{s}}\text{COO}^-$) is larger than that observed for ionic compounds. (ii) when $\Delta\nu$ is considerably smaller than that for ionic compounds, the carboxylate group coordinated with metal ions as a bidentate feature. In case of the value of $\Delta\nu$ same as observed in ionic compounds this means that the carboxylate group acts as bridged. Based on these facts it is possible to distinguish the coordination mode of the COO^- group (Refat et al., 2006).

Gluconic acid exhibits a strong absorption band around 1735 cm^{-1} due to the $\nu(\text{C}=\text{O})$ of carboxylic group this band is absent in case of aluminum compound. Concerning the aluminum gluconate compound formed, the difference between the asymmetrical and symmetrical vibrations ($\nu_{\text{as}} - \nu_{\text{s}} = 150 \text{ cm}^{-1}$) existed in Table 1 is larger than the data recorded for HG. This assumption strongly suggests that COO^- group is acting as a monodentate ligand (type I).

The $\text{Al(G)}_3 \cdot 10\text{H}_2\text{O}$ complex exhibits a strong absorption band around 295 nm. The obtained spectrum is shown in Fig. 3. The molar absorptivity (ϵ_{max}) of the aluminum gluconate compound is $9430 \text{ l mol}^{-1} \text{cm}^{-1}$. This value is almost three times than that of gluconic acid ($3220 \text{ l mol}^{-1} \text{cm}^{-1}$) at a concentration $10^{-4} \text{ mol l}^{-1}$, in agreement with the fact that three gluconate moieties are coordinated to aluminum nucleus.

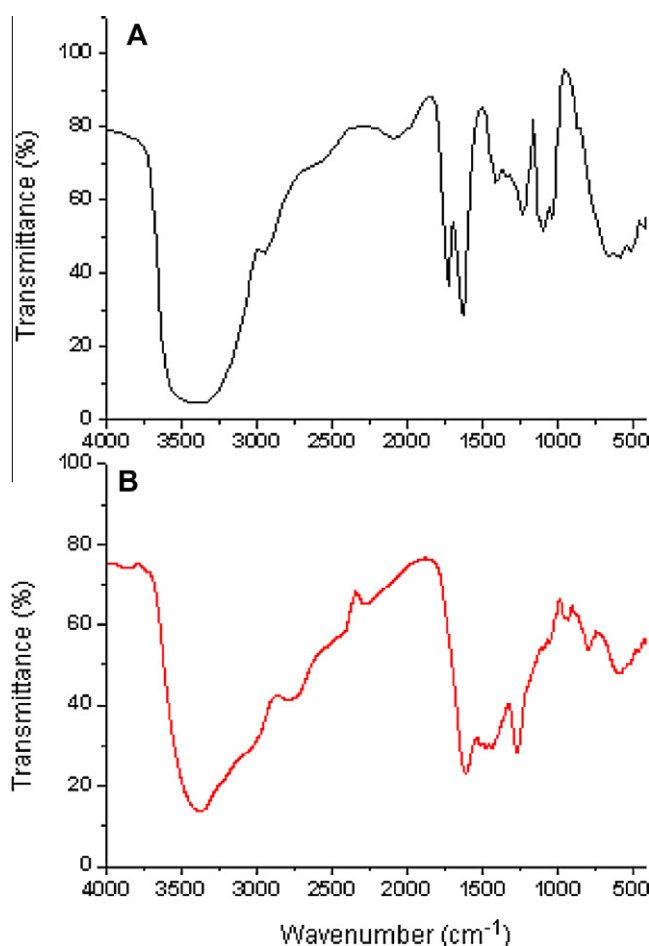


Figure 2 Infrared spectra of (A) HG and (B) $\text{Al(G)}_3 \cdot 10\text{H}_2\text{O}$ complex.

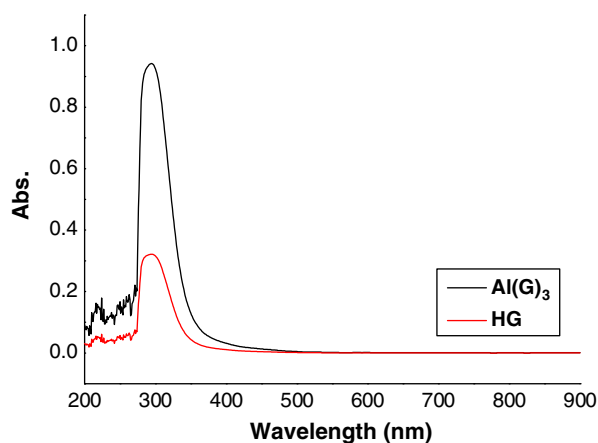


Figure 3 Electronic spectra of (A) HG and (B) Al(G)₃ complex.

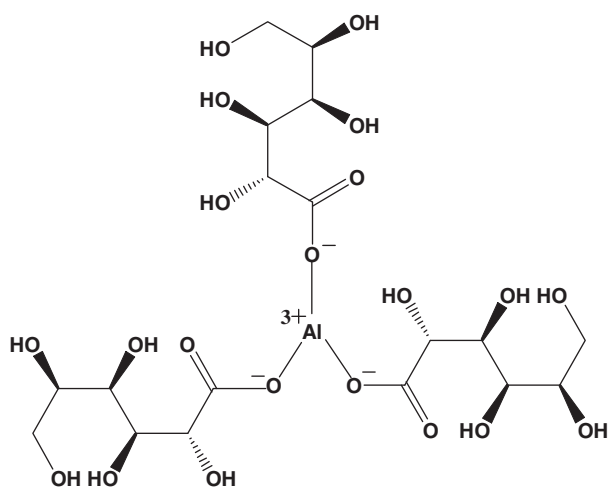


Figure 4 The proposed structure of Al-G⁻ complex.

Based on the above interpretation aluminum gluconate can be designed as shown in Fig. 4.

3.2. Photo-inhibition of localized attack

3.2.1. Cyclic polarization measurements

Fig. 5 shows cyclic potentiodynamic polarization curves recorded for Al in 0.25 M HG at 25 °C under the conditions of continuous illumination at 300 nm and non-illumination. A total of four plots are shown (two representative plots for the non-illumination conditions and two for the illumination conditions) to illustrate the degree of reproducibility from experiment to experiment. It seems that the reproducibility of the polarization curves is good.

It is evident that illumination leads to a considerable reduction in the anodic current at applied potentials exceeding 0.0 V(SCE). The pitting potential depended slightly on illumination, while the repassivation (protection) potential was found to be completely independent on illumination. An anodic displacement in the pitting potential of 70 ± 20 mV was observed on continuous illumination. This displacement ΔE_{pit} ($\Delta E_{\text{pit}} = E_{\text{pit}}^{(\text{light})} - E_{\text{pit}}^{(\text{dark})}$) was evaluated from a total of 20 experiments, 10 carried out in the dark and 10 performed under continuous illumination conditions. The data presented show that the resistance of Al to localized attack in HG solutions can be enhanced on illuminating the immersed electrodes with UV light. Although illumination has only a small effect on the potential at which passivity breakdown is first observed, illumination decreases considerably the rate at which further sites become activated. This means that illumination under these conditions has a little influence on pit initiation and a significant effect on pit propagation.

In order to correlate this current–potential behavior with the nature of the surface attack, a number of experiments were carried out in which the electrode was polarized up to a predetermined potential, then removed from the solution and the surface viewed under a high resolution optical microscope. These experiments were carried out for both illuminated and non-illuminated specimens. Localized attack was observed

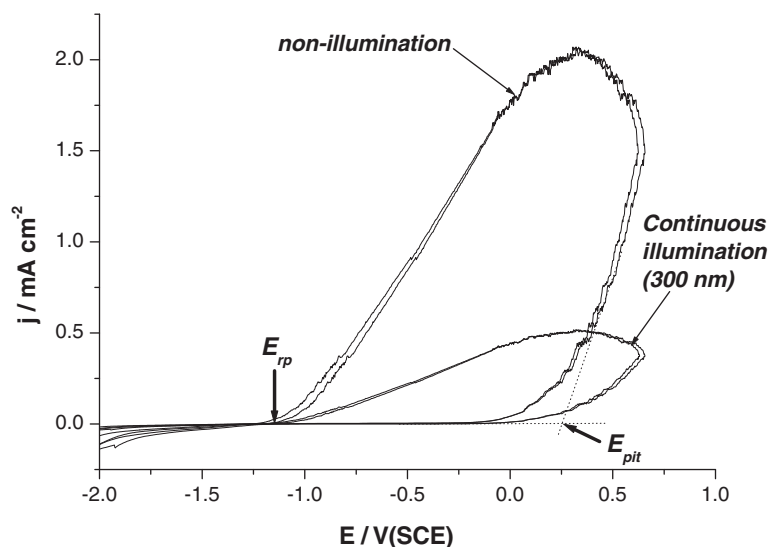


Figure 5 Cyclic polarization curve recorded for Al in 0.25 M HG at a scan rate of 0.2 mV s^{-1} at 25 °C under the conditions of continuous illumination (300 nm) and non-illumination.

following the initial current increase. On continued polarization, a greater number of initiation sites could be seen and eventually the attack spread over the surface. But, the rate at which this attack spreads to damage the surface was reduced on illumination.

The polarization behavior was found to vary only slightly with photon energy. In Fig. 6, the polarization plots, recorded for Al in 0.25 M HG solution, are shown as a function of wavelength. Here, it is seen that increasing the wavelength to 400 nm, decreases only marginally the resistance to anodic dissolution afforded by illumination (i.e., little influence on pit nucleation and marked suppression on its propagation and growth).

It can be seen from the data presented that illumination of the surface during the polarization measurements is sufficient to induce changes in the passive film that render it more resistant to attack. This, coupled with the fact that illumination seemed to have little effect on the rate of pit nucleation, suggests that the observed enhanced resistance to the localized attack is associated with some modification of the passive film that exists under these conditions (passivation-induced photo effect).

It is well-known that the composition and development of passive layers on metals and alloys is dependent on parameters such as the applied potential, pH, time of formation, sample composition, etc. It is also known that the pitting susceptibility of the metals and alloys depends on the nature of the passive film. In addition, variations in the manner in which the film is grown affect the passivity breakdown process and initiation of pitting attack. Thus, it is possible that the observed photo-induced passivation effect may be connected with alterations in the composition of the passive film where these alterations or modifications are facilitated or accelerated by illuminating the electrode.

Following Breslin and Macdonald (1998), on illuminating semiconductor oxide films with sufficiently energetic photons, electrons are promoted from the valence to the conduction band generating electron-hole pairs or electron-ionized center pairs. These electron-hole pairs become separated with the holes and electrons moving in opposite directions. This separation of charge gives rise to a counter field, so that the electric field strength within the passive layer is quenched. This situation persists only while the electrode is illuminated, but this

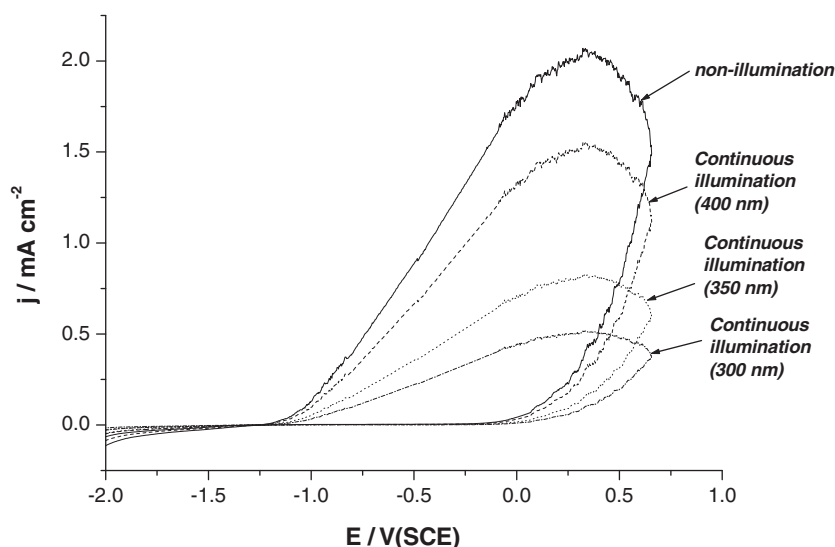


Figure 6 Cyclic polarization curve recorded for Al in 0.25 M HG at a scan rate of 0.2 mV s^{-1} at 25°C under the conditions of continuous illumination (300–400 nm) and non-illumination.

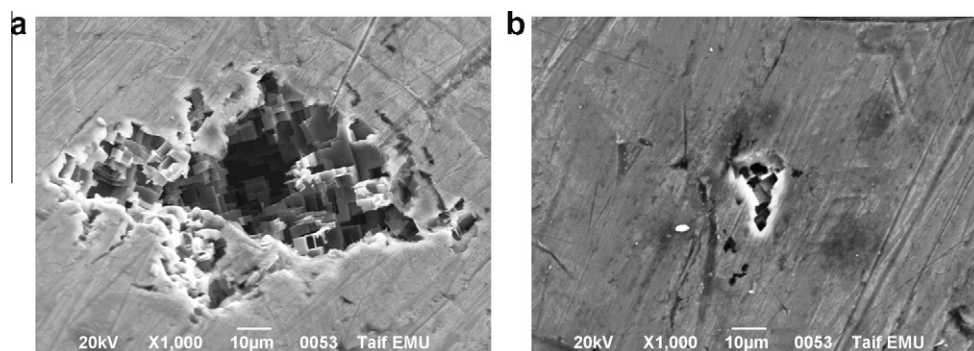


Figure 7 SEM micrographs recorded for Al in 0.25 M HG solution under galvanostatic regime at 0.20 V under the conditions of non-illumination (image a) and continuous illumination at 300 nm of the incident UV light (image b). The electrode was held for 5.0 min at the specified potential.

process is predicted (Macdonald, 1992) to modify the vacancy structure, which is much slower to relax. Since this modification of the vacancy structure depends on the quenching of the electric field strength (Macdonald, 1992), it is justified to postulate that the fundamental origin is quenching of the electric field strength. The effects of a decrease in the electric field strength on the susceptibility of the passive film to undergo localized attack can be seen from equations presented in the work of Breslin and Macdonald (1998).

3.2.2. Morphology of pitting as a function of energy of photons

Fig. 7 presents SEM micrographs recorded for non-illuminated (image a) and illuminated (300 nm) (image b) Al electrode immersed in 0.25 M HG solution at 25 °C. It is quite clear that the surface morphology varies upon illumination. Severe pitting attack is observed in the absence of light (see image a). On the other hand, the corroded areas obviously diminished upon illumination.

4. Conclusions

The anodic and corrosion behavior of Al were studied in gluconic acid (HG) solutions under different experimental conditions based on cyclic polarization measurements. It is found that Al suffers from pitting corrosion in HG solutions. Pitting corrosion occurs as a result of adsorption of gluconate anions (G^-) on the passive surface and their reaction with Al^{3+} in the oxide lattice to form soluble $Al-G^-$ complex species ejected into the solution by diffusion. Complexation of Al(III) with the aggressive G^- anion was elucidated using elemental analysis, IR-spectroscopy and UV-vis spectra. The infrared spectral data are in agreement with coordination through carboxylate-metal, with G^- acting as a monodentate ligand.

The influence of UV light (300–450 nm) on the passive and dissolution behavior of Al in 0.25 M HG solution was also studied. On illuminating the immersed electrode a slight ennoblement in the pitting potential was observed. A significant decrease in the anodic current at potentials exceeding the pitting potential was also observed. These findings were explained in terms of a photo-induced quenching of the electric field strength and a consequent modification of the vacancy structure within the passive films, which accounts for the observed photo-inhibition of passivity breakdown. SEM examinations of the pitted surface revealed that pitting attack is suppressed on illumination.

References

- Abdel Rehim, S.S., Hassan, H.H., Amin, M.A., 2002. Galvanostatic anodization of pure Al in some aqueous acid solutions Part I: Growth kinetics, composition and morphological structure of porous and barrier-type anodic alumina films. *J. Appl. Electrochem.* 32, 1257.
- Amin, M.A., Abd El Rehim, S.S., El-Lithy, A.S., 2010a. Pitting and pitting control of Al in gluconic acid solutions—Polarization, chronoamperometry and morphological studies. *Corros. Sci.* 52, 3099.
- Amin, M.A., Abd El Rehim, S.S., El-Lithy, A.S., 2010b. Corrosion, passivation and breakdown of passivity of Al and Al–Cu alloys in gluconic acid solutions. *Electrochim. Acta* 55, 5996.
- Belca, I.D., Zekovic, Lj.D., Jovanic, B., Ristovski, G., Ristovski, Lj., 2000. The theory of galvanoluminescence in the anodic oxide films obtained by aluminum anodization in ammonium tartrate. *Electrochim. Acta* 45, 4095.
- Breslin, C.B., Macdonald, D.D., 1998. The influence of UV light on the dissolution and passive behavior of copper-containing alloys in chloride solutions. *Electrochim. Acta* 44, 643.
- Brown, G.E., 1999. Metal oxide surfaces and their interactions with aqueous solutions and microbial organisms. *Chem. Rev.* 99, 77.
- Bocchetta, P., Sunseri, C., Bottino, A., Capannelli, G., Chiavarotti, G., Piazza, S., Di Quarto, F., 2002. Asymmetric alumina membranes electrochemically formed in oxalic acid solution. *J. Appl. Electrochem.* 32, 977.
- Deacon, G.B., Phillips, R.J., 1980. Relationships between the carbon-oxygen stretching frequencies of carboxylate complexes and the type of carboxylate coordination. *Coord. Chem. Rev.* 33, 227.
- Diglee, J.W., Downie, T.C., Goulding, C.W., 1969. Anodic Aluminum Oxide Templates for Nanocapacitor Array Fabrication. *Chem. Rev.* 69, 365.
- Galvele, J.R., 1976a. In: Staehle, R.W., Okada, H. (Eds.), *Passivity and Its Breakdown on Iron and Iron Base Alloys*. NACE, Houston, TX, pp. 118–120.
- Galvele, J.R., 1976b. Transport processes and the mechanism of pitting of metals. *J. Electrochem. Soc.* 123 (4), 464.
- Garcia-Vergara, S.J., Skeldon, P., Thompson, G.E., Habazaki, H., 2008. Behaviour of a fast migrating cation species in porous anodic alumina. *Corros. Sci.* 50, 3179.
- Hohl, H., Stumm, M., 1976. Interaction of Pb^{2+} with hydrous $\gamma-Al_2O_3$. *J. Colloid Interface Sci.* 55, 281.
- Ikonopisov, S., 1975. Problems and contradictions in galvanoluminescence, a critical review. *Electrochim. Acta* 20, 783.
- Ikonopisov, S., Elenkov, N., Klein, E., Andreeva, L., 1978. Galvanoluminescence of aluminium during anodization in non-dissolving electrolytes. *Electrochim. Acta* 23, 1209.
- Jackson, N.F., Cambell, D.S., 1976. Thin films in electrolytic capacitors. *Thin Solid Films* 36, 331.
- Keitelman, A.D., Gravano, S.M., Galvele, J.R., 1984. Localized acidification as the cause of passivity breakdown of high purity zinc. *Corros. Sci.* 24 (6), 535.
- Kim, Y.-S., Pyun, S.-I., Moon, S.-M., Kim, J.-D., 1996. The effects of applied potential and pH on the electrochemical dissolution of barrier layer in porous anodic oxide film on pure aluminium. *Corros. Sci.* 38, 329.
- Macdonald, D.D., 1992. The point defect model for the passive state. *J. Electrochem. Soc.* 139, 3434.
- Nagayama, M., Tamura, K., Takahashi, H., 1972. Mechanism of open-circuit dissolution of porous oxide films on aluminium in acid solutions. *Corros. Sci.* 12, 133.
- Pakes, A., Thompson, G.E., Skeldon, P., Morgan, P.C., 2003. Development of porous anodic films on 2014-T4 aluminium alloy in tetraborate electrolyte. *Corros. Sci.* 45, 1275.
- Refat, M.S., Nandan Kumar, Deo, de Farias, Robson F., 2006. Spectroscopic and thermal investigations of Cu(II), Zn(II), Cd(II), Pb(II) and Al(III) caproates. *J. Coord. Chem.* 59 (16), 1857.
- Shimizu, K., Tajima, S., 1980a. Theory of electroluminescence of Al/anodic alumina/electrolyte system. *Electrochim. Acta* 24, 309.
- Shimizu, K., Tajima, S., 1980b. Localized nature of the luminescence during galvanostatic anodizing of high purity aluminium in inorganic electrolytes. *Electrochim. Acta* 25, 259.
- Stojadinovic, S., Belca, I., Kasalic, B., Zekovic, Lj., Tadic, M., 2006. The galvanoluminescence spectra of barrier oxide films on aluminum formed in inorganic electrolytes. *Electrochem. Commun.* 8, 1621.
- Suay, J.J., Giménez, E., Rodríguez, T., Habbib, K., Saura, J.J., 2003. Characterization of anodized and sealed aluminium by EIS. *Corros. Sci.* 45, 611.
- Szklarska-Smialowska, Z., 1986. *Pitting Corrosion of Metals*. NACE, Houston, TX.
- Tajima, S., 1977. Luminescence, breakdown and colouring of anodic oxide films on aluminium. *Electrochim. Acta* 22, 995.
- Tajima, S., Shimizu, K., Baba, N., Matsuzawa, S., 1977a. Nature of luminescence during galvanostatic anodizing of high purity aluminium. *Electrochim. Acta* 22, 845.

- Tajima, S., Shimizu, K., Baba, N., Matsuzawa, S., 1977b. Effect of crystal orientation on galvanoluminescence of aluminium. *Electrochim. Acta* 22, 851.
- van Geel, W.Ch., Pistorius, C.A., Bouma, B.C., 1957. Luminescence of the oxide layer on Aluminum during and after its formation by electrolytic oxidation. *Philips Res. Rep.* 12, 465.
- Wernick, S., Pinner, R., Sheasby, P.G., 1987. *The Surface Treatment and Finishing of Aluminum and Its Alloys*, fifth ed. Finishing Publication Ltd., Teddington, Middlesex, UK.
- Wood, R., Fornasiero, D., Ralston, J., 1990. Electrochemistry of the boehmite–water interface. *Colloids Surf.* 51, 389.